High-speed imaging of glutamate release with genetically encoded sensors

Céline D. Dürst[1], J. Simon Wiegert[1a], Nordine Helassa[2b], Silke Kerruth[2c], Catherine Coates[2], Christian Schulze[1], Michael Geeves[3], Katalin Török[2] and Thomas G. Oertner[1]*

[1]Institute for Synaptic Physiology, Center for Molecular Neurobiology Hamburg, Hamburg 20251, Germany

[2]Molecular and Clinical Sciences Research Institute, St George's, University of London, London SW17 0RE, UK

[3]School of Biosciences, University of Kent, Canterbury CT2 7NZ, UK

[a]Present address: Research Group Synaptic Wiring and Information Processing, Center for Molecular Neurobiology Hamburg, Hamburg 20251, Germany

[b]Present address: Department of Cellular and Molecular Physiology, Institute of Translational Medicine, University of Liverpool, L69 3BX Liverpool, United Kingdom

[c]Present address: Department of Biophysical Chemistry, J. Heyrovský Institute of Physical Chemistry, Dolejškova 2155/3, 182 00 Prague, Czech Republic

*corresponding author: thomas.oertner@zmnh.uni-hamburg.de

KEYWORDS: genetically-encoded glutamate indicator, GEGI, glutamate, two-photon imaging, two-photon microscopy, synaptic transmission, stopped-flow, iGluSnFR, hippocampal culture, rat, pyramidal cell, CA1, excitatory synapse, multivesicular release, organotypic culture, single-cell electroporation.

EDITORIAL SUMMARY This Protocol describes the design, *in vitro* characterisation and imaging applications of iGluSnFR-based genetically-encoded glutamate indicators (GEGIs) in tissue culture of rat hippocampus

TWEET A new protocol for the design, characterisation and high-speed imaging applications of genetically-encoded glutamate indicators (GEGIs).

COVER TEASER High-speed imaging of glutamate release

Up to three primary research articles where the protocol has been used and/or developed.

1. Helassa, N. et al. Ultrafast glutamate sensors resolve high-frequency release at Schaffer collateral synapses. Proc. Natl. Acad. Sci. U. S. A. 115, 5594–5599 (2018).

2.

3.

31 **Abstract**

32 The strength of an excitatory synapse depends on its ability to release glutamate and on the density of
33 postsynaptic receptors. Genetically-encoded glutamate indicators (GEGIs) allow eavesdropping on
34 synaptic transmission at the level of cleft glutamate to investigate properties of the release machinery in
35 detail. Based on the sensor iGluSnFR, we recently developed accelerated versions that allow
36 investigating synaptic release during 100 Hz trains. Here we describe the detailed procedures for design
37 and characterization of fast iGluSnFR variants *in vitro*, transfection of pyramidal cells in organotypic
38 hippocampal cultures, and imaging of evoked glutamate transients with two-photon laser scanning
39 microscopy. As the released glutamate spreads from a point source - the fusing vesicle - it is possible to
40 localize the vesicle fusion site with a precision exceeding the optical resolution of the microscope. By
41 using a spiral scan path, the temporal resolution can be increased to 1 kHz to capture the peak of fast
42 iGluSnFR transients. The typical time frame for these experiments is 30 min per synapse.

Introduction

One of the fundamental parameters setting synaptic strength is the release probability of the presynaptic bouton. Release probability is classically assessed in electrophysiological recordings from the postsynaptic neuron. In neocortex and hippocampus, however, two neurons are frequently connected by more than one synapse, which makes it very difficult to achieve a situation where responses from a single synapse can be electrophysiologically isolated. Furthermore, both presynaptic changes (vesicle depletion, changes in release probability) and changes on the level of postsynaptic receptors (e.g., phosphorylation, desensitization, saturation, lateral diffusion, and internalization) contribute to the variability of postsynaptic responses [1,2]. These effects become even more difficult to disentangle during high-frequency stimulation, when all physiological parameters change simultaneously as the synapse struggles to maintain transmission. Due to these complications, it is an attractive proposition to assess synaptic physiology with functional imaging methods, as they convincingly isolate responses from a single synapse even if other synapses on the same neuron are active at the same time. While a large number of imaging studies used postsynaptic Ca^{2+} transients as a read-out of synaptic efficacy, it is now possible to intercept synaptic transmission at the level of cleft glutamate, effectively isolating presynaptic dynamics from postsynaptic changes.

Overview of optical glutamate sensors

In the last decade, two types of optical glutamate sensors have been developed: chemically-labeled and genetically-encoded glutamate indicators (GEGIs). Both types of sensors utilize a glutamate-binding protein which is either labeled with a synthetic fluorophore or fused to a fluorescent protein. Sensors based on the ligand-binding domain of AMPAR subunit conjugated with a small fluorescent dye molecule near the glutamate-binding pocket have been used to image bulk extrasynaptic glutamate dynamics in the brain [3,4]. A chemical FRET-based approach, combining a donor and acceptor fluorophore with the glutamate binding protein iGluR5-S1S2 (Snifit-iGluR5) [5] showed an improved fluorescence change in cultured cells but has not been applied to brain tissue yet. Sparse and cell-specific labeling without background fluorescence, a precondition for single-synapse studies, seems to be difficult to achieve with chemically labeled sensors.

The first fully genetically-encoded glutamate indicator (GEGI) called FLIPE [6] was FRET-based and contained a glutamate binding protein (GltI from *E.coli*) located between an N-terminal enhanced cyan fluorescent protein (ECFP) and a C-terminal yellow fluorescent protein called Venus. Later improved to reach a maximum CFP/YFP ratio change of 44% and a K_d of 2.5 µM (Hires et al., 2008), the sensor named SuperGluSnFR allowed measurements of the time course of synaptic glutamate release and spillover in hippocampal cultures. However, the signal-to-noise ratio (SNR) of SuperGluSnFR was still low, and ~30 traces had to be averaged to measure glutamate release in response to single action potentials. A significant improvement was the development of iGluSnFR [9]. iGluSnFR is an intensity-based glutamate sensor constructed from *E. coli* GltI and circularly permuted (cp) EGFP. Its high fluorescence dynamic range ($\Delta F/F_{max}$ of 4.5) and K_d of ~4 µM make it a very suitable tool for investigating cleft glutamate dynamics. iGluSnFR has been used to measure glutamate in a variety of tissues such as the retina [10], visual cortex [11] and olfactory bulb [12]. We and others developed variants displaying different kinetics, affinities and emission profiles [13–15]. Those new GEGIs with varied biophysical properties enable

83   researchers to select the most appropriate sensor depending on the biological question (bulk tissue vs.
84   single synapse) and imaging system (camera, galvanometric laser scanner, or resonant scanner).

Comparison with other methods to image presynaptic function

86   To image presynaptic function, fluorescent glutamate sensors are not the only possibility. The change in
87   vesicular pH during vesicle exocytosis and recycling/reacidification has been successfully exploited to
88   measure the activity of individual presynaptic terminals. Synapto-pHIuorin, the first genetically-encoded
89   pH indicator, was based on a pH-sensitive GFP variant fused to the C-terminus of synaptobrevin/VAMP2
90   (vesicular associated membrane protein-2) to target the sensor to the inner surface of synaptic vesicles
91   [16]. Other vesicular targeting strategies used fusion to synaptophysin [17], synaptotagmin [18] and the
92   vesicular glutamate transporter VGLUT [19]. Spectrally red-shifted sensors with a red fluorescent pH-
93   sensitive protein like VGLUT-mOrange2 [20] and sypHTomato [21] were developed, and the ratiometric
94   sensor Ratio-sypHy [22] was instrumental in revealing the arrested development of synapses in dissociated
95   neuronal culture. In addition, in primary cultures, pHluorins are sufficiently sensitive to detect single
96   vesicle release events [23–25]. It is even possible to localize individual fusion events with a precision
97   exceeding the resolution limit of the microscope [26]. Analysis of release during high-frequency activity,
98   however, is difficult with pH-based methods: reuptake and reacidification are slow processes, leading to
99   rapid accumulation of green fluorescence inside active synaptic terminals. Furthermore, pH-based
100   indicators provide no information about the glutamate content (filling state) of individual vesicles.
101   Another technique to study presynaptic function is to image the loading and unloading of amphiphilic
102   styryl dyes (FM dyes), initially developed to study vesicle recycling at the neuromuscular junction (NMJ)
103   [27]. The lack of cellular selectivity prevents the use of FM dyes at individual synapses in the densely
104   packed neuropil. In addition, the relatively long partitioning time of FM dyes in- and out of the
105   membrane (seconds) renders the relation between staining/destaining events and sub-millisecond
106   glutamate release rather obscure.

Overview of the Procedure

108   The Procedure can be divided into two sections (see Fig. 1); sensor development (Steps 1-42) and
109   functional imaging of synaptic activity in hippocampal slice cultures (Steps 43-62).
110   **Sensor development (Steps 1-42):** While iGluSnFR is an excellent general-purpose GEGI, it may be
111   necessary to further optimize specific properties such as affinity for glutamate (K_d), brightness, or
112   kinetics for specific experiments. Optimization starts with structure-guided mutations of residues
113   close to the glutamate binding pocket (Fig. 1a) (Step 1). Newly generated variants are expressed in *E.*
114   *coli*, purified and tested *in vitro* for glutamate-induced changes in fluorescence (Steps 2-20). If the
115   dynamic range is deemed sufficient, affinity and kinetics are determined by stopped-flow fluorimetry
116   (Steps 21-37). The most promising candidates are expressed and characterized in HEK cells (Steps 38-
117   42) and finally, in neurons (Steps 43-62). We found considerable differences in the absolute affinity
118   and kinetics of sensor molecules in solution compared to the same molecules tethered to the plasma
119   membrane of cells [13]. Relative differences between GEGIs, however, were conserved, validating the
120   use of *in vitro* calibrations for sensor optimization.
121   **Imaging synaptic function (Steps 43-62):** Single-cell electroporation is the method of choice to
122   achieve very sparse expression of glutamate sensors in organotypic culture of brain tissue (Fig. 1b)

123 (Steps 46-56). The sparse expression makes it easy to follow the axon of a patch-clamped sensor-
124 expressing neuron to a distal projection area, e.g., CA1. While camera-based systems are ideal for
125 functional imaging in dissociated neuronal culture, two-photon microscopy is typically used to detect
126 weak functional signals deep in scattering tissue (Steps 57-62). The optimal strategy for functional
127 imaging depends on the goal of the experiment: to obtain spatial information about the fusion sites
128 of vesicles on individual presynaptic boutons, we use fast frame scans and slower GEGIs (iGluSnFR)
129 (Step 62 Option A). To accurately determine the amplitude of individual glutamate transients, a
130 prerequisite for optical quantal analysis, spiral scans on individual boutons provide increased
131 temporal resolution and better signal-to-noise ratio (SNR) (Step 62 Option B). While 500 Hz provide
132 sufficient temporal resolution for iGluSnFR imaging, we increase the spiral scan frequency to 1 kHz
133 for ultrafast GEGIs.

Limitations of the method

135 Glutamate diffuses out of the synaptic cleft in less than 1 ms. Even the fastest GEGIs cannot monitor the
136 true kinetics of free glutamate diffusion as the sensor needs time to rearrange its conformation to
137 become fluorescent. In addition, scanning microscopy has limited temporal resolution. For capturing
138 sub-millisecond fluorescence changes, it would be necessary to park the excitation beam on the synaptic
139 cleft. This is not a technical problem, but in practice, point-scan experiments are extremely sensitive to
140 small lateral movements of the active bouton in the tissue. At the moment, galvanometric scanning can
141 still adequately sample the fastest GEGIs.

142 The number of trials that can be obtained from a single bouton is limited by the unavoidable bleaching of
143 the indicator molecules and eventual destruction of the release machinery by toxic photoproducts (e.g.,
144 oxygen radicals). Therefore, the laser exposition per single AP should be reduced to a minimum. To
145 measure GEGI transients in response to individual APs, we image in spiral mode for ~ 80 ms. We
146 routinely acquire ~100 trials from single boutons without any decay in amplitude or release probability
147 (see Experimental design and Supplemental Fig. 1c). By using lower laser power, this number can be
148 extended to 200 trials at the cost of a slightly lower SNR. Longer intervals between trials allow
149 replenishing indicator molecules by lateral diffusion, but this strategy is limited by the need for stable
150 whole-cell access during the entire experiment for reliable action potential generation.

Experimental design

152 **Development and characterization of fast glutamate probes:** Site-directed mutagenesis and protein
153 expression/purification are done following standard procedures and should lead to high yields of the
154 GEGIs with a purity > 90% in a single-step purification process (determined by SDS-PAGE). One of the
155 most important parameters is the fluorescence dynamic range (F_{+glu} - F_{-glu} / F_{-glu}) which is a measure of the
156 fluorescence change upon glutamate binding. If the dynamic range of the new GEGI variant is < 2, the
157 probe's response to glutamate is not high enough to be suitable for cellular experiments.

158 The affinity of the GEGI, expressed as K_d, has to be appropriate for the expected glutamate concentration
159 in the cellular or tissue environment. If the goal of the experiment is to distinguish synaptic failures (no

160 glutamate release, no GEGI signal) from successes (stimulation-induced glutamate release), a very high
161 affinity is desirable. If a linear response is important, e.g., to estimate the number of vesicles released
162 simultaneously, a slightly lower affinity might be advantageous. For a GEGI to be a useful probe for *in*
163 *vivo* imaging, it also needs to be specific for glutamate. Therefore, binding to other ligands has to be
164 assessed (Fig. 2a). As iGluSnFR is based on the glutamate/aspartate ABC transporter protein (Gltl), it is
165 expected that the sensor retains a significant affinity for aspartate. However, it should be unresponsive
166 to serine or glutamine. Most of the GEGIs indeed show a fluorescence response to aspartate binding,
167 sometimes even with higher fluorescence dynamic range than for glutamate. However, the affinity is
168 often lower, and fortunately, aspartate does not act as a neurotransmitter. Nevertheless, aspartate
169 sensitivity needs to be considered when monitoring glutamate in non-neuronal tissues or cellular
170 compartments.

171 To observe fast events like neurotransmission in synapses, the kinetics of the formation and decay of the
172 fluorescence state are critical. Thus, the association and dissociation of the purified GEGIs are
173 determined *in vitro* by stopped-flow fluorimetry (Fig. 2b). While performing association measurements,
174 it is essential to record baselines for the buffer to obtain the zero level of the PMT and for the glutamate-
175 free GEGI to obtain the starting point of the fluorescence increase. This recording is essential to detect
176 rapid phases ($>1000 \text{ s}^{-1}$) that are faster than the resolution of the stopped-flow device (about 1 ms
177 mixing time) and thus appear as jumps. Recording the dissociation of glutamate from the GEGIs is
178 especially challenging, as the glutamate needs to be removed from the sensor, which is difficult due to
179 lack of chemical traps. We circumvent this obstacle by mixing the glutamate-bound GEGI with the high
180 affinity GluBP 600n (K_d about 600 nM) [6]. However, for low affinity variants, these measurements are
181 limited by the concentration of GluBP 600n available and by the very small decrease in fluorescence
182 amplitude. Low-affinity GEGIs ($K_d > 1$ mM) have to be saturated with glutamate concentrations in the
183 mM range, however, GluBP 600n is at best concentrated to be ~ 1 mM in the optical cell. As only a small
184 fraction of the GEGI is dispossessed of its glutamate, only a very small decrease in fluorescence occurs
185 and, thus a small signal is observed.

186 For *in vivo* use of the GEGIs, the sensors need to be attached to the outer membrane of a cell. Thus, the
187 sensors are cloned in mammalian expression vectors, which add a mouse Ig κ-chain for secretion and a
188 PDGFR transmembrane helix for membrane attachment. In order to confirm correct localization, the
189 sensor is expressed in cell lines (HEK293T cells) and titrated with glutamate to determine the cellular K_d.
190 We found that the attachment to the outer membrane of the cell increases the variants' affinity for
191 glutamate by a factor of up to 20-fold. Relative differences between the variants, however, are
192 conserved [13]. This affinity increase needs to be considered when choosing a suitable sensor for *in vivo*
193 applications.

194 **Imaging synaptic glutamate release with two-photon microscopy:** For expression in neurons, we clone
195 the GEGIs behind the human synapsin 1 promoter and electroporate single neurons in organotypic slice
196 cultures of rat hippocampus. GEGIs are relatively dim in the absence of glutamate, making it difficult to
197 focus on small structures such as axonal boutons. We routinely use co-expression of a bright red
198 fluorescent protein (tdimer2 or tdTomato) to label the cytoplasm and follow the axon through the tissue;
199 the newly developed CyRFP1 [28] is also an excellent choice for this purpose. The red fluorescence also

200   provides additional information about the volume of individual boutons. Electroporated CA3 neurons are
201   clearly visible under a stereomicroscope (5x objective, DsRed filter set) 2-4 days after electroporation
202   (Fig. 3a-c). Two-photon excitation at 980 nm reveals axons and boutons of the expressing neurons in CA1
203   *stratum radiatum*, far away from the somata in CA3 (Fig. 3c). Targeted patch-clamp recording from a
204   transfected neuron allows triggering single action potentials (APs) by brief depolarizing current injections
205   (Fig. 3e). Simultaneous imaging of a single bouton (spiral scan path at high zoom (Fig. 5a-c)) reveals green
206   fluorescence transients time-locked to the action potentials, indicating glutamate release from the
207   stimulated bouton. In spite of reliable action potential generation, synapses frequently failed to release
208   glutamate (Fig. 3e, gray traces), indicating a stochastic vesicle fusion process.

209   **Fusion site localization:** While spiral scans are optimal to determine the peak amplitude of the
210   glutamate signal, we use fast frame scans (16 x 16 pixels, frame rate 62.5 Hz) to localize the likely
211   location of the fusing vesicle in individual trials. The spatial peak of the averaged signal does not
212   necessarily occur in the center of the bouton, but often close to the edge (Fig. 4b), reflecting the random
213   orientation of the synaptic cleft on the surface of the bouton. To localize individual fusion events in noisy
214   images, we fit a two-dimensional Gaussian kernel (Fig. 4c) to the first frame after stimulation. Plotting
215   the center positions of Gaussian fits (Fig. 4c) relative to the morphological outline of the bouton (red
216   channel) revealed a small region of release, the active zone (Fig. 4d). Increasing the extracellular Ca^{2+}
217   concentration from 1 mM to 4 mM did increase the amplitude of single-trial responses, but not the size
218   of the apparent active zone (Fig. 4e). The higher cleft glutamate concentrations caused by single action
219   potentials in 4 mM Ca^{2+} suggest the simultaneous release of multiple vesicles or a switch from partial to
220   full release. No clustering was found when we fitted green fluorescence before stimulation or in trials
221   classified as failures (Fig. 4f and g).

222   **Spiral scans and amplitude extraction:** As we do not know a priori where on the bouton the highly
223   localized and short-lived GEGI signals will appear (Fig. 5a), we need to sample the entire surface of the
224   bouton as fast as possible. Traditional raster scanning (Fig. 5b) requires extreme acceleration of the
225   scanning mirror at the end of every scan line, limiting the maximum frame rate to ~120 Hz. By scanning a
226   spiral pattern, we are able to sample the same area at frequencies up to 1 kHz. The point spread function
227   (PSF) of our two-photon microscope is 0.5 μm in the imaging plane and 1.7 μm along the optical axis
228   (FWHM, measured with 170 nm fluorescent beads). As the PSF is elongates in the axial direction, we
229   sample the upper and lower surface of the bouton simultaneously. Our goal is to extract the amplitude
230   of fluorescent transients from spiral scans independent of the exact position of the fusion site on the
231   bouton. To do so, the unfolded spiral scans are plotted as straight lines underneath each other, resulting
232   in a space-time plot (Fig. 5c). Typically, the spiral scan intersects the diffusing cloud of glutamate two or
233   three times per scan, resulting in multiple 'hot spots' that all contained information about the same
234   release event. To extract amplitude information, columns (corresponding to positions on the bouton) are
235   sorted according to the change in fluorescence (Fig. 5d). The columns with the largest signal ($\Delta F >$
236   $\Delta F_{max}/2$) are averaged (region of interest, ROI). In trials where no fluorescence change is detected
237   (failures), the same columns as in the last 'success' trial are analyzed. As opposed to a static region-of-
238   interest (ROI), this analysis procedure is robust against minute drift of the tissue between trials and does
239   not require a priori knowledge of the fusion location. We extract the amplitude from the resulting
240   fluorescence trace by fitting a single exponential function to the decay of the fluorescence transient. To

241 estimate the noise level (photon shot noise) in every experiment, we perform the same fitting procedure
242 to a section of the baseline (before stimulation). As expected, the baseline amplitudes are close to zero
243 (Fig. 5f, gray dots and columns). Typically, the histogram of all responses (green) also show one cluster
244 around zero (failures of release), the remaining responses (successes) form an asymmetric, broad peak
245 between 40 and 160% $\Delta F/F_0$. A close inspection of the spatial distribution of the signal (Fig. 5e, average
246 of 10 successes) shows a rapid decay of the peak, but no lateral spread as might be expected from a
247 diffusion process. It is important to note that the diffusion of free glutamate out of the synaptic cleft
248 happens in less than 1 ms and cannot be resolved by iGluSnFR or another GEGI. Instead, what we
249 observe is the relatively slow unbinding of glutamate from quasi-stationary iGluSnFR molecules,
250 explaining the lack of lateral spread of the signal.
251

252 **Materials**

253 **Reagents**
254 • Plasmids
255 o pCMV iGluSnFR (Addgene plasmid #41732) [9], iGluSnFR in mammalian expression vector,
256 can be used for expression in HEK293T cells and as starting point for SDM to induce new
257 mutations
258 o pET41a(+) (Novagen, Merck cat. no. 70556-3), bacterial expression vector used to
259 express GEGI variants in *E. coli*
260 o pET30b (Merck cat. no. 69909), bacterial expression vector used to express GEGI variants
261 in *E. coli*
262 o pCI syn iGluSnFR (Addgene plasmid #106123), mammalian expression vector to express
263 iGluSnFR in neurons (hippocampal slices)
264 o pDisplay FLIPE-600n (Addgene plasmid # 13545) [6], vector encoding for GluBP 600n for
265 expression of glutamate-binding protein GluBP 600n in *E. coli*. Purified GluBP is used for
266 kinetic analysis *in vitro*.
267 o pCI syn iGlu$_f$ (Addgene plasmid #106121)[13], mammalian expression vector for expression
268 of iGlu$_f$ in neurons
269 o pCI syn iGlu$_u$ (Addgene plasmid #106122)[13], mammalian expression vector for expression
270 of iGlu$_u$ in neurons
271 o pCI syn tdimer2, a gift of Roger Y. Tsien [29], mammalian expression vector for expression
272 of dimeric red fluorescent protein in neurons
273 • Cloning and molecular biology
274 o Restriction enzymes: BglII, NotI (NEB cat. no. R0144 and R0189)
275 o T4 DNA ligase (NEB cat. no. M0202)
276 o QuikChange XL Site-Directed Mutagenesis Kit (Agilent Technologies cat. no. 200516)
277 o NucleoSpin® Plasmid kit (Machery and Nagel cat. no. 740588)
278 o HiSpeed Plasmid Midi Kit (Qiagen cat. no. 12643)
279 o LB Broth (Powder) - Lennox (Fisher BioReagents cat no. BP1427)
280 o LB Agar, Lennox (Granulated) (Fisher BioReagents cat no. BP9745)
281 o Kanamycin sulfate (Fisher BioReagents cat no. BP906)

282   **CAUTION**: toxic. Wear protective gloves, clothing, and eye protection. Wash hands
283   thoroughly after handling.
284   ○ PureLink HiPure Plasmid Maxiprep (Life Technologies cat. no. K210006)
285 • General reagents
286   ○ HEPES (Fine White Crystals/Molecular Biology) (Fisher Scientific cat. no. BP310-1)
287   ○ Sodium chloride, BioXtra, ≥99.5% (AT) (Merck cat. no. S7653)
288   ○ 1 M $MgCl_2$ solution (Invitrogen AM9530G)
289   ○ Sodium hydroxide (Merck cat no. S8045)
290   **CAUTION**: Danger. Corrosive to metals and causes severe skin burns and eye damage.
291   Wear protective gloves, clothing, and eye protection. Wash hands thoroughly after
292   handling.
293   ○ D(+)-Glucose (Merck cat no. D9434)
294   ○ Potassium chloride, BioXtra, ≥99.0% (Merck cat no. P9333)
295   ○ NaH_2PO_4 (Merck cat no. S0751)
296 • Protein expression and purification
297   ○ Pierce™ Protease Inhibitor Tablets, EDTA-free (Thermo Fisher Scientific cat. no. A32965)
298   **CAUTION**: Danger, causes severe skin burn and eye damage. Wear protective gloves,
299   clothing and eye protection. Wash hands thoroughly after handling.
300   **CRITICAL**: EDTA-free inhibitor is critical to ensure binding of the His tagged protein to the
301   HisTrap High Performance column
302   ○ HisTrap™ High Performance (GE Healthcare cat. no. 17524801)
303   ○ SnakeSkin™ Dialysis Tubing, 3.5K MWCO, 22 mm (Thermo Fisher Scientific cat. no.
304   68035)
305 • Glutamate, aspartate, and serine titration
306   ○ L-Glutamic acid (Merck cat. no. G1251)
307   ○ L-Aspartic acid (Merck cat. no. A8949)
308   ○ L-Serine (Merck cat. no. S4500)
309 • Testing in cell lines
310   ○ HEK293T cells (Merck cat. no. 85120602)
311   **CAUTION**: The cell lines used in your research should be regularly checked to ensure
312   they are authentic and are not infected with mycoplasma.
313   ○ Sensorplate, 24 well, PS, F-bottom, glass bottom, black, lid, sterile, single packed
314   (Greiner bio one cat. no. 662892)
315   ○ DMEM, high glucose, GlutaMAX™ Supplement, pyruvate (Gibco, Thermo Fisher Scientific
316   cat. no. 31966047)
317   ○ MEM Non-Essential Amino Acids Solution (100X) (Gibco, Thermo Fisher Scientific cat. no.
318   11140035)
319   ○ Fetal Bovine Serum (FBS), qualified, heat inactivated, E.U.-approved, South America
320   Origin (Gibco, Thermo Fisher Scientific cat. no. 10500056)
321   ○ Penicillin-Streptomycin (10,000 U/mL) (Gibco, Thermo Fisher Scientific cat. no.
322   15140122)

323			**CAUTION**: Causes skin irritation, eye irritation, may cause an allergic skin reaction and

323   **CAUTION**: Causes skin irritation, eye irritation, may cause an allergic skin reaction and

324   respiratory irritation. Wear protective gloves, clothing, and eye protection. Wash hands

325   thoroughly after handling.

326   o Lipofectamine™ 2000 Transfection Reagent (Thermo Fisher Scientific cat. no. 11668027)

327   • Slice culture and recording

328   o Slice cultures from rodent hippocampus [30]

329   **CAUTION**: Any experiments involving live rats must conform to relevant Institutional and

330   National regulations. In our case, organ explant procedures were approved by the

331   veterinary of the University Medical Center Hamburg-Eppendorf, Germany

332   o MEM (Sigma-Aldrich cat. no. M7278)

333   o Heat-inactivated horse serum (Gibco cat. no. 16050-122)

334   o L-glutamine (200 mM; Gibco cat. no. 25030-024)

335   o L-ascorbic acid (Sigma-Aldrich, cat. no. A5960)

336   o Insulin (1 mg/mL; Sigma-Aldrich cat. no. I1882)

337   o HEPES (Sigma-Aldrich cat. no. H4034)

338   o K-gluconate (Sigma-Aldrich, cat. no. G4500)

339   o EGTA (Sigma-Aldrich, cat. no. E0396)

340   o Na_2-ATP (Sigma-Aldrich, cat. no. A3377)

341   o Na-GTP (Sigma-Aldrich, cat. no. G8877)

342   o Na_2-phosphocreatine (Sigma-Aldrich, cat. no. P7936)

343   o $NaHCO_3$ (Sigma-Aldrich, cat. no. S5761)

344   o NaH_2PO_4 (Sigma-Aldrich, cat. no. S5011)

345   o Potassium chloride (Sigma-Aldrich, cat. no. S5886)

346   o 1 M KCl (Fluka cat. no. 60121)

347   o 1 M $MgSO_4$ (Fluka cat. no. 63126)

348   o 1 M $MgCl_2$ (Fluka, cat. no. 63020)

349   o 1 M $CaCl_2$ (Fluka cat. no. 21114)

350   o D-glucose (Fluka cat. no. 49152)

351   o Cl_3Fe (Fluka cat. no. 10695862)

352 **Reagent Setup**

353   **Resuspension buffer for expression:** 50 mM HEPES-Na^+, 200 mM NaCl, pH 7.5, filtered (0.2 μm

354   pore size) and stored at 4°C for 2 weeks

355   **Elution buffer for expression:** 50 mM HEPES-Na^+, 200 mM NaCl, 500 mM imidazole, pH 7.5,

356   filtered (0.2 μm pore size) and stored at 4°C for 2 weeks

357   **Storage buffer for expression:** 50 mM HEPES-Na^+, 100 mM NaCl, pH 7.5, stored at 4°C for 2

358   weeks

359   **Assay buffer for biophysical characterization:** 50 mM HEPES-Na^+, 100 mM NaCl, 2 mM $MgCl_2$,

360   pH 7.5, stored at 4°C for 2 weeks

361   **Association buffers for biophysical characterization:**

362	• 1 µM GEGI in assay buffer, stored at 4°C for one day.
363	• 0.1x K_d to 10x K_d glutamate in assay buffer, stored at 4°C for one day
364	CRITICAL: In order to measure the full range of response in dependence of the glutamate
365	concentration, the glutamate concentration mixed with the GEGI has to be distributed around
366	the K_d

367 **Dissociation buffers for biophysical characterization:**

368 • 2 mM GluBP 600n in assay buffer, stored at 4°C for one day.
369 • 1 µM GEGI in assay buffer, stored at 4°C for one day.
370 • 1 µM GEGI in assay buffer with saturating glutamate (10x K_d), stored at 4°C for one day

371 **Complete DMEM:** DMEM, 1x NEAA, 10% (v/v) FBS, 100 U/ml penicillin-streptomycin, stored at
372 4°C for 2 month.

373 **HEK293T cell imaging buffer:** 20 mM HEPES-Na$^+$, 145 mM NaCl, 10 mM glucose, 5 mM KCl, 1 mM
374 MgCl$_2$, 1 mM NaH$_2$PO$_4$, pH 7.4 stored at 4°C for up to 6 month.

375 **Slice culture medium:** 394 ml MEM, 20% (v/v) Heat-inactivated horse serum, 1 mM L-glutamine,
376 0.01 mg/ml Insulin, 14.5 mM NaCl, 2 mM MgSO$_4$, 1.44 mM CaCl$_2$, 0.00125% Ascorbic acid, 13 mM
377 D-glucose. Medium has to be sterile filtered (0.2 µm pore size) and stored at 4°C for up to 4
378 weeks.

379 **Slice culture transduction solution:** 10 mM HEPES, 145 mM NaCl, 25 mM D-glucose, 2.5 mM KCl,
380 1 mM MgCl$_2$, 2 mM CaCl$_2$. Measure the pH using a pH-meter and adjust to pH 7.4 by adding
381 NaOH or HCl. Measure the osmolality with a micro-osmometer and ensure that the osmolality is
382 between 310-320 mOsm/kg. If the osmolality is out of range, a mistake was made during
383 solution preparation. Solution has to be sterile filtered (0.2 µm pore size), stored at 4°C for up to
384 6 months and pre-warmed to 37°C before use.

385 **Recording solution, artificial cerebrospinal fluid (ACSF):** 25 mM NaHCO$_3$, 1.25 mM NaH$_2$PO$_4$, 127
386 mM NaCl, 25 mM D-glucose, 2.5 mM KCl, 2 mM CaCl$_2$, 1 mM MgCl$_2$, pH adjusted to 7.4, ACSF has
387 to be saturated with 95% O$_2$ and 5% CO$_2$. Osmolality should be between 310-320 mOsm/kg.
388 Store for max. 1 week at 4°C. Bubble with Carbogen (95% O$_2$, 5% CO$_2$) during warm-up to
389 prevent Ca^{2+} precipitation. Maintain perfusion reservoir at 34°C to prevent bubble formation in
390 recording chamber.

391 **K-gluconate-based intracellular solution:** 10 mM HEPES, 135 mM K-gluconate, 0.2 mM EGTA, 4
392 mM MgCl$_2$, 4 mM Na$_2$-ATP, 0.4 mM Na-GTP, 10 mM Na$_2$-phosphocreatine, 3 mM L-ascorbic acid,
393 pH adjusted to 7.2 with KOH. Osmolality should be between 290-300 mOsm/kg. Solution has to
394 be sterile filtered (0.2 µm pore size), stored at -20°C. Aliquot in Eppendorf tubes can be stored at
395 -80°C for max. 6 months. Store on ice during the experiment to slow down ATP hydrolysis.

396 **Equipment**
397 • Equipment for protein expression/purification

398   o   Sonicator for lysing *E. coli* (Sonics & Materials Inc., VibraCell)

399   o   ÄKTA Purifier or Explorer (GE healthcare)

400   •   Equipment for biophysical characterization

401   o   Fluorescence spectrometer with magnetic stirring function (Fluorolog3, Horiba Scientific)

402   o   Hellma® fluorescence cuvettes, ultra Micro (Merck, cat. no. Z802336-1EA)

403   o   Hellma fluorescence cuvette QS 3500 µL (Merck, cat. no. Z600172-1EA)

404   o   ALADDIN syringe pump (World Precision Instruments, cat. no. AL-1000)

405   o   SGE syringe 250 µL, barrel inner diameter 2.30 mm (Trajan Scientific and Medical, cat.
406   no. P/N 006230)

407   o   'KinetAsyst' Dual-mixing Stopped-Flow System (TgK Scientific, cat. no. SF-61DX2)
408   equipped with two circulating water baths for temperature control and a long-pass filter
409   >530 nm. The equipment should be set up in a dark lab with red light illumination and
410   temperature control (20°C)

411   •   Equipment for imaging in cell lines

412   o   Inverted spinning-disk confocal fluorescence microscope (3i Marianas)

413   •   Electrophysiology equipment

414   o   pE-4000 LED light source (CoolLED) for epifluorescence

415   o   infrared Dodt contrast (Luigs & Neumann)

416   o   Patch-clamp amplifier (Axon Instruments, model no. MultiClamp 700B)

417   o   Microelectrode manipulator (Sutter Instrument, MP-285).

418   o   Micropipettes for whole-cell recording (Borosilicate glass with filament, 1.5 mm O.D.)

419   •   Electroporation equipment

420   o   Upright microscope with a motorized stage, CCD camera and IR-DIC (infrared differential
421   interference contrast) or Dodt contrast

422   o   20x water immersion objective (Zeiss Achroplan)

423   o   4x zoom lens system (0.5 – 2.0x magnification range)

424   o   Vibration isolation table (Table Stable LTD, TS-150)

425   o   Axoporator 800A with HL-U pipette holder (Molecular Devices)

426   o   Plastic syringe body (1 ml) as disposable mouthpiece, connected through a Luer 1-way
427   stopcock and thin silicone tubing to the electrode holder

428   o   Headphones and speakers

429   o   Microscope chamber made of a glass microscope slide (70 x 100 x 1 mm) onto which a
430   Teflon ring (inner diameter: ~ 35 mm, height: 2 mm) is fixed with silicone aquarium
431   sealant

432   o   Motorized micromanipulators (Luigs & Neumann)

433   o   Silver wire (diameter: ~ 0.25 mm)

434   o   Forceps (Fine Science Tools, cat. no. 11002-16)

435   o   Hot bead sterilizer (Fine Science Tools, cat. no. 18000-45)

436   o   Incubator (37°C; 5% CO_2) with rapid humidity recovery and copper chamber (Heracell
437   150i/160i, Thermo Scientific)

438   o   Micropipette puller (PC-10, Narishige)

439   o   Thin-walled borosilicate glass capillaries (WPI, cat. no. TW150F-3)

440   ○   Tissue culture dishes (60 mm, sterile; Sarstedt, cat. no. 83.1801)

441   ○   Ultrafree centrifugal filter units (Millipore, cat. no.UFC30GV0S)

442   ○   Micro-osmometer (Fiske Model 210)

443   **CRITICAL**: The electroporation microscope should be situated close to the tissue culture

444   hood (in the same room) to prevent contamination. We built a laminar flow cabinet with

445   HEPA filter unit around the electroporation setup. The microscope has to be

446   mechanically isolated from the vibrations generated by the fan in the filter box; we use

447   an active anti-vibration table.

448   •   Software

449   ○   ImageJ2 (https://imagej.net/ImageJ2)

450   ○   GraphPad Prism 7 (https://www.graphpad.com/)

451   ○   ScanImage 3.8 [31] (https://vidriotechnologies.com/)

452   ○   Ephus [32] (https://www.janelia.org/open-science/ephus)

453   **Equipment Setup**

454   ○   **Equipment for functional imaging in tissue:** We built a two-photon microscope based on

455   an Olympus BX51WI microscope with pE-4000 LED light source (CoolLED) for

456   epifluorescence and infrared Dodt contrast (Luigs & Neumann). A Ti:Sapphire laser

457   system with dispersion compensation (MaiTai DeepSee, Spectra Physics) was coupled in

458   through an electro-optical modulator (EOM, Conoptics), a 3x telescope (Thorlabs), 5 mm

459   scan mirrors (Cambridge), a compound scan lens (f = 50 mm [33]), a dual camera port with

460   IR mirror (Olympus) and a water immersion objective (LUMPLFLN 60XW, 60x, NA 1.0,

461   Olympus). Red and green fluorescence was detected through the objective and the oil

462   immersion condenser (NA 1.4, Olympus) using 2 pairs of photomultiplier tubes (H7422P-

463   40SEL, Hamamatsu). 560 DXCR dichroic mirrors and 525/50 and 607/70 emission filters

464   (Chroma Technology) were used to separate green and red fluorescence. Excitation light

465   was blocked by short-pass filters (ET700SP-2P, Chroma). During epifluorescence

466   illumination, sub-stage PMTs were protected by a NS45B shutter (Uniblitz). For electrical

467   stimulation of individual neurons, we mounted the head-stage of a MultiClamp 700B

468   amplifier (Molecular Devices) on a MP-285 micromanipulator (Sutter Instruments) on a

469   motorized stage (40-40, Danaher Motion) that also moved the perfusion chamber

470   (quartz glass bottom). Temperature was controlled by Peltier-heating of the oil-

471   immersion condenser and in-line heating of the perfusion solution (Warner Instruments).

472   The setup was controlled by Matlab software (ScanImage [31] and Ephus [32]) via data

473   acquisition boards (National Instruments). At the start of a trial, electrophysiology and

474   image acquisition were synchronized by a hardware trigger (TTL pulse). During a trial (2 s,

475   typically), laser power was regulated via EOM and restricted to the periods of expected

476   glutamate release (20 - 80 ms window, depending on GEGI kinetics) to minimize

477   bleaching.

478   **CRITICAL**: To minimize bleaching by excessive excitation, the microscope has to be

479   designed to detect emitted photons very efficiently. Using only the objective for

480 fluorescence detection is not sufficient to achieve single-vesicle sensitivity. Condenser
481 detection (oil-immersion, 1.4 NA, large field of view) is essential for the success of single
482 synapse experiments with many trials. Replace aging PMTs with excessive dark counts.

483 **CRITICAL:** The oil-immersion condenser has to be permanently heated (day and night) if
484 a recording temperature above room temperature is desired. This can be achieved with
485 flexible heating pads or Peltier elements. As the thermal mass of the condenser is very
486 large, constant-current heating is sufficient, provided that the temperature of the
487 perfusion solution is additionally regulated by a feedback control circuit (in-line heater,
488 Warner Instruments). A climate chamber would be an attractive solution but is not
489 compatible with direct-mounted PMTs.

490 **CRITICAL:** If a galvanometric scanning system is used, the microscope software has to
491 support arbitrary line scans or spiral scans[34]. The code for arbitrary line scans that we
492 developed for our original study is now incorporated in the ScanImage software (Version
493 2016 and later). ScanImage is developed and supported by Vidrio Technologies, LLC as an
494 open-source research resource. A resonant scanning system may be sufficiently fast in
495 frame mode if extreme zoom-in (few scan lines) can be realized.

496 ## Procedure

497 **Generation of GEGIs** Timing 1 week (5 h hands-on time)
498 **CRITICAL**: We have made a number of GEGI-encoding plasmids available via Addgene (see Reagents).
499 Follow Steps 1-42 in order to design GEGIs with tailored biophysical parameters.

1. Analyze protein 3D structures of the 99% homolog of GltI of *Shigella flexneri* (PDB 2VHA) and
   literature [35,36] to assign critical residues involved in glutamate binding. Substitute essential
   residues with amino acids with similar physical properties. Avoid radical changes in amino acid
   size or charge as this will frequently result in misfolded or otherwise non-functional proteins.
2. Subclone the iGluSnFR gene from a mammalian expression vector into a bacterial expression
   vector (pET41a) using restriction digestion of BglII and NotI and ligation (T4 DNA ligase) following
   the manufacturer's protocol.
   CAUTION: Subcloning requires DNA to be analyzed by agarose gels. This requires the use of DNA
   intercalating fluorescent dyes (e.g. ethidium bromide or Sybr green) which highly toxic as
   mutagens and should be handled with care. DNA imaging systems are based on UV lamps so
   appropriate personal protective equipment should be used.
3. Insert point mutations using the QuikChange XL site-directed mutagenesis kit following the
   manufacturer's instructions and confirm new variants by DNA sequencing.
4. Subclone *glti* gene encoding GluBP 600n from pRSET FLIPE 600n (ECFP-ybeJ-Venus) into pET30b
   (His-fusion expression vector) at BglII and NotI restriction sites.

515 **Expression and purification of new GEGIs** Timing 3 days (10 h hands-on time)

516	5.	Transform 1 μL of iGluSnFR variants or GluBP 600n plasmid DNA into 50 μL of _E. coli_ BL21 (DE3)
517		gold chemically competent cells.
518	6.	Pick one colony and grow in 10 mL LB-medium supplemented with 100 μg/mL kanamycin for
519		overnight at 37°C and 180 rpm (pre-culture).
520	7.	Inoculate 1 L LB-medium containing 100 μg/mL kanamycin with whole pre-culture, incubate at
521		37°C and 180 rpm until OD_{600} reaches (0.6-0.8).
522	8.	Cool the cells down to 20°C.
523	9.	Induce protein expression with 0.5 mM Isopropyl β-D-1-thiogalactopyranoside (IPTG) and
524		incubate at 20°C and 180 rpm overnight.

525 **CRITICAL STEP:** Best protein yields are obtained when inducing expression during exponential
526 phase of growth (OD_{600} 0.6-0.8), overnight at 18-20 °C.
527 10. Harvest cells by centrifugation at 3000 _g_ for 15 min at room temperature, resuspend cells in
528 40 mL resuspension buffer supplemented with Pierce Protease Inhibitors and lyse via sonication
529 on ice for 2 min (2 sec "on" and 8 sec "off").
530 **CAUTION**: Wear ear protection equipment during sonication.
531 **CRITICAL STEP**: Sonication produces heat and may result in the degradation of your protein of
532 interest. Performing sonication on ice and in the presence of protease inhibitors will dramatically
533 limit this phenomenon.
534 11. Remove the cell debris by ultracentrifugation at 100,000 _g_ for 45 min at 4°C.
535 **CRITICAL STEP:** After cell lysis, all steps are performed at 4°C when possible to avoid protein
536 digestion by cellular proteases (steps 12-14).
537 12. Load the supernatant on equilibrated HisTrap HP column (nickel affinity resin) mounted on an
538 ÄKTA system (flow rate 4 mL/min) and wash with 40 mL resuspension buffer.
539 13. Elute the protein with 10 column volumes of a linear gradient of resuspension and elution buffer
540 (0 to 0.5 M imidazole) and collect in 2 mL fractions. Analyze the purified protein by SDS-PAGE
541 and stain the gel with Coomassie blue.
542 14. Pool fractions of interest and dialyze overnight at 4°C in a snakeskin dialysis tubing (3.5 kDa)
543 against 4 L storage buffer.
544 **CRITICAL STEP:** It is essential to perform dialysis to remove the imidazole from your buffer.
545 Otherwise, protein precipitation will occur upon defrosting (from step 15). The dialysis
546 molecular weight cut-off used can be higher than 3.5 kDa as long as it is below 15 kDa.
547 15. Store purified protein in fractions of 1 mL in the -80°C freezer.
548 **PAUSE POINT:** The purified protein can be stored at -80°C for up to 3 years.

549 **Determining the dynamic range** Timing 1 h
550 16. Prepare 50-100 nM iGluSnFR proteins in assay buffer, add to a Hellma micro cuvette (50 μL) and
551 place the cuvette into a fluorescence spectrometer pre-equilibrated to 20 °C.
552 17. Record the fluorescence emission spectrum (λ_{ex} = 492 nm and λ_{em} = 497-550 nm) (F_{-glu}).
553 18. Add 10 mM glutamate solution to the micro cuvette, mix well and record the fluorescence
554 emission spectrum (λ_{ex} = 492 nm and λ_{em} = 497-550 nm) (F_{+glu}).
555 19. To analyze the data, take the maximal emission (around 514 nm) of each measurement and
556 calculate the fluorescence dynamic range ((F_{+glu}- F_{-glu})/F_{-glu}).

516 5. Transform 1 μL of iGluSnFR variants or GluBP 600n plasmid DNA into 50 μL of _E. coli_ BL21 (DE3)
517 gold chemically competent cells.
518 6. Pick one colony and grow in 10 mL LB-medium supplemented with 100 μg/mL kanamycin for
519 overnight at 37°C and 180 rpm (pre-culture).
520 7. Inoculate 1 L LB-medium containing 100 μg/mL kanamycin with whole pre-culture, incubate at
521 37°C and 180 rpm until OD_{600} reaches (0.6-0.8).
522 8. Cool the cells down to 20°C.
523 9. Induce protein expression with 0.5 mM Isopropyl β-D-1-thiogalactopyranoside (IPTG) and
524 incubate at 20°C and 180 rpm overnight.
525 **CRITICAL STEP:** Best protein yields are obtained when inducing expression during exponential
526 phase of growth (OD_{600} 0.6-0.8), overnight at 18-20 °C.
527 10. Harvest cells by centrifugation at 3000 _g_ for 15 min at room temperature, resuspend cells in
528 40 mL resuspension buffer supplemented with Pierce Protease Inhibitors and lyse via sonication
529 on ice for 2 min (2 sec "on" and 8 sec "off").
530 **CAUTION**: Wear ear protection equipment during sonication.
531 **CRITICAL STEP**: Sonication produces heat and may result in the degradation of your protein of
532 interest. Performing sonication on ice and in the presence of protease inhibitors will dramatically
533 limit this phenomenon.
534 11. Remove the cell debris by ultracentrifugation at 100,000 _g_ for 45 min at 4°C.
535 **CRITICAL STEP:** After cell lysis, all steps are performed at 4°C when possible to avoid protein
536 digestion by cellular proteases (steps 12-14).
537 12. Load the supernatant on equilibrated HisTrap HP column (nickel affinity resin) mounted on an
538 ÄKTA system (flow rate 4 mL/min) and wash with 40 mL resuspension buffer.
539 13. Elute the protein with 10 column volumes of a linear gradient of resuspension and elution buffer
540 (0 to 0.5 M imidazole) and collect in 2 mL fractions. Analyze the purified protein by SDS-PAGE
541 and stain the gel with Coomassie blue.
542 14. Pool fractions of interest and dialyze overnight at 4°C in a snakeskin dialysis tubing (3.5 kDa)
543 against 4 L storage buffer.
544 **CRITICAL STEP:** It is essential to perform dialysis to remove the imidazole from your buffer.
545 Otherwise, protein precipitation will occur upon defrosting (from step 15). The dialysis
546 molecular weight cut-off used can be higher than 3.5 kDa as long as it is below 15 kDa.
547 15. Store purified protein in fractions of 1 mL in the -80°C freezer.
548 **PAUSE POINT:** The purified protein can be stored at -80°C for up to 3 years.

549 **Determining the dynamic range** Timing 1 h
550 16. Prepare 50-100 nM iGluSnFR proteins in assay buffer, add to a Hellma micro cuvette (50 μL) and
551 place the cuvette into a fluorescence spectrometer pre-equilibrated to 20 °C.
552 17. Record the fluorescence emission spectrum (λ_{ex} = 492 nm and λ_{em} = 497-550 nm) (F_{-glu}).
553 18. Add 10 mM glutamate solution to the micro cuvette, mix well and record the fluorescence
554 emission spectrum (λ_{ex} = 492 nm and λ_{em} = 497-550 nm) (F_{+glu}).
555 19. To analyze the data, take the maximal emission (around 514 nm) of each measurement and
556 calculate the fluorescence dynamic range ((F_{+glu}- F_{-glu})/F_{-glu}).

557   20. Repeat Steps 16-19 twice in order to generate 3 independent replicates.

558   **CRITICAL STEP:** If the fluorescence dynamic range is < 2 the fluorescence change upon glutamate

559   binding is too low for imaging in hippocampal slices. In that case, try using higher concentrations

560   of glutamate. If the fluorescence dynamic range has not improved, return to the "Selection of

561   residues close to binding pocket step" and select another mutation.

562 **Determining K_d and specificity** Timing 2 h for each ligand

563   21. Prepare 50-100 nM GEGI in 3 mL assay buffer in a 3500 µL Hellma Quartz cuvette (QS).

564   22. Add a magnetic stir bar and place the cuvette into spectrofluorometer.

565   **CRITICAL STEP:** Make sure stir bar is moving rigorously.

566   23. Fill a 250 µL Hamilton syringe with assay buffer with appropriate ligand: L-glutamate (10x K_d 10-

567   50 mM), L-aspartate (10x K_d 10-50 mM) or L-serine (10x K_d 10-50 mM).

568   **CRITICAL STEP:** Make sure there are no air bubbles in the syringe nor in the tubing.

569   24. Install the syringe in an Aladdin syringe pump, set the flow rate to 10 µL/min and place the

570   tubing outlet carefully into the micro cuvette.

571   25. Simultaneously start the recording of the fluorescence emission over time (λ_{ex} = 492 nm and

572   λ_{em} = 514 nm) and the syringe pump.

573   26. To analyze the data, use time information to calculate the ligand concentration in the cuvette at

574   each given time point. Correct the fluorescence emission for dilution/photobleaching and

575   normalize it. Plot the corrected and normalized fluorescence against the ligand concentration

576   and fit with a Hill equation for specific binding (GraphPad Prism 7) to obtain affinity for

577   glutamate (K_d) and cooperativity of binding (n).

578   27. Repeat Steps 21-26 twice in order to generate at least 3 independent experiments.

579 **Measuring kinetics** Timing 5 h (4h for association, 1h for dissociation)

580   **CRITICAL:** Temperature control is essential for all kinetic measurements. Furthermore, washing the

581   instrument firmly after changing the ligand concentration is critical. To correctly analyze the data

582   baselines and maximum fluorescence intensity lines should be recorded as described below. Always

583   average at least five records ("shots") for each measurement to obtain a representative trace.

584   28. ***Association (Steps 28-32):*** Mix 1 µM GEGI in assay buffer with the maximal glutamate

585   concentration in assay buffer (10x K_d, as determined in Step 27). Set the fluorescence level after

586   mixing to reach 80% detector saturation by adjusting the gain on the PMT (reference of 1 for

587   normalization). This step will prevent detector overload in future experiments.

588   29. Mix assay buffer with assay buffer and record the baseline (reference of 0 for normalization).

589   30. Mix 1 µM GEGI in assay buffer with assay buffer. This measurement should result in a straight

590   line and shows the basal fluorescence without ligand bound.

591   **CRITICAL STEP:** Steps 28-30 need to be performed before starting any association kinetic

592   measurement of a GEGI. It ensures that the instrument is calibrated for maximum/minimum

593   fluorescence detection levels and prevents detector damage.

594   31. Glutamate dependent association kinetics: Mix 1 µM iGluSnFR variant in assay buffer with

595   increasing glutamate concentrations in assay buffer (0.1x to 10x K_d). Record and average five

596   measurements for each glutamate concentration.

597		CRITICAL STEP: You may have to perform measurements of different time scales to have enough
598		data points for an accurate exponential fitting. Make sure you use about 10 different glutamate
599		concentrations to measure the fluorescence increase with increasing glutamate and also the
600		saturation as shown by reaching a maximum in fluorescence and on-rate.
601	32.	To analyze the data, normalize the recorded time traces to the PMT baseline and the maximal
602		fluorescence level. Fit the time traces with mono- or biexponential decays (Kinetic studio or
603		GraphPad Prism 7). Plot the obtained observed rate constants against the glutamate
604		concentration.
605		
606	33.	***Dissociation (Steps 33-37):*** Mix 1 µM GEGI in glutamate saturating assay buffer (10x K_d, as
607		determined in Step 27) with the same buffer. Set the fluorescence level after mixing to reach
608		80% detector saturation by adjusting the gain on the PMT (reference of 1 for normalization). This
609		step will prevent detector overload in future experiments.
610	34.	Perform step 29 to obtain the reference for 0.
611	35.	Perform step 30 to obtain the basal fluorescence level.
612		CRITICAL STEP: Steps 34-35 need to be performed before starting any dissociation kinetic
613		measurement of a GEGI. It ensures that the instrument is calibrated for maximum/minimum
614		fluorescence detection levels and prevents detector damage.
615	36.	Dissociation kinetics: Mix 1 µM GEGI in assay buffer with saturating glutamate concentration
616		(10x K_d) with 2 mM GluBP 600n in assay buffer. Higher concentrations of GluBP 600n are not
617		advisable as precipitation might occur. Record and average five measurements.
618		CRITICAL STEP: You may have to perform measurements of different time scale to have enough
619		data points for an accurate exponential fitting.
620	37.	To analyze the data, normalize the recorded time traces to the PMT baseline and the maximum
621		fluorescence level. Then fit the time trace with mono- or biexponential decays (Kinetic studio or
622		GraphPad Prism 7). Plot the obtained observed rate constants against the glutamate
623		concentration.

Determining fluorescence dynamic range and K_d in HEK293T cells Timing 2 days (5 h hands-on time)

626	38.	Seed ~200,000 cells onto 24-well glass bottom fluorescence plates in complete DMEM and let
627		them attach for 24 h in the incubator (37°C, 5% (v/v) CO_2).
628	39.	Transfect the cells with GEGI plasmids generated by SDM of promising mutations into the
629		mammalian expression vector pCMV iGluSnFR using Lipofectamine 2000 following the
630		manufacturer's protocol.
631	40.	Examine the cells 24 h post-transfection at 37 °C with a confocal microscope (light source
632		488 nm, using GFP settings). Check for localization at the plasma membrane.
633	41.	Glutamate titration: add stepwise glutamate to final concentrations between 0-10x K_d (as
634		determined in Step 27) and take an image of the cells before and after each addition step.
635		CRITICAL STEP: Focus drift may happen when you add glutamate. If it is the case, discard the last
636		data-point and move to a different well.
637	42.	Define elliptical regions of interest (ROI) along cell membrane and determine the fluorescence
638		intensity (ImageJ). Normalize intensity for each individual cell and average over a total number

639   of >20 cells. Plot relative intensity versus glutamate concentration and fit data with Hill equation
640   (GraphPad Prism 7).

641 **Cloning in neuronal expression vector** Timing 7 days (5h hands-on time)
642   43. Use QuikChange XL site-directed mutagenesis kit to insert mutation of promising GEGI variants
643   into pCI syn iGluSnFR vector and confirm by DNA sequencing.
644   44. Prepare plasmid for electroporation using a plasmid DNA preparation kit (e.g. PureLink HiPure
645   Maxiprep kit from Life Technologies)

646 **Culture preparation** Timing 15 min/brain
647   45. Prepare organotypic slice cultures (rat hippocampus)as described in [30].

648 **Single-cell electroporation** Timing 10 min plus 10-20 min per slice, depending on slice quality and
649 number of cells to transfect
650   46. ***Preparation of plasmids and DNA (Steps 46-47):*** Sterile filter an aliquot (0.5 ml) of K-gluconate-
651   based intracellular solution through a Millipore Ultrafree centrifugal unit by centrifugation at
652   16,000 g for several seconds in a table-top centrifuge at 4°C.
653   47. Add the GEGI plasmids to the desired concentration after removal of the filter insert. Use 40 to
654   50 ng/μL for pCI syn iGlu$_f$ (Addgene plasmid #106121) or pCI syn iGlu$_u$ (Addgene plasmid
655   #106122) [13]. For different cell types and GEGIs, the final concentration may have to be
656   determined empirically (range: 1-100 ng/μL).
657   CRITICAL STEP: It is important that the DNA-containing solution is not passed through the
658   Millipore Ultrafree centrifugal filter unit.
659   CRITICAL STEP: To aid visualization of axons and boutons of transfected neurons, mix plasmid
660   encoding for red fluorescent protein (e.g. tdimer2; 20 ng/μL) with GEGI plasmid to achieve co-
661   expression.
662
663   PAUSE POINT: The electroporation solution containing the plasmid can be stored between
664   electroporation sessions at -20°C for up to 1 year.
665
666   48. ***Electroporation (Steps 48-56):*** Coat silver wires tips and ground electrodes with AgCl by bathing
667   them in a saturated Cl$_3$Fe solution for at least 30 min or overnight prior to first use.
668   49. Pull electroporation pipettes using a micropipette puller (e.g. PC-10, Narishige). Pull thin-walled
669   borosilicate capillaries to obtain a resistance of 10-15 MΩ when filled with the intracellular
670   solution.
671   CRITICAL STEP: Ensure constant pipette resistance for reproducible expression. A too high
672   pipette resistance leads to low expression, whereas a too low resistance causes extreme
673   expression levels and toxicity.
674   50. Back-fill an electroporation pipette with ~1.2 μL of plasmid mix solution (from Step 47) for each
675   slice to electroporate. Back-filled pipettes can be kept (in an upright position) for up to 2 hours
676   before use. Pipette 1 mL of transduction solution (37˚C) into the microscope chamber. Transfer
677   one slice culture insert into the chamber (sterile forceps) and add transduction solution on top of

678	the slice culture for the water immersion objective. Use a sterile 60-mm dish to cover the
679	microscope chamber to transfer to the microscope to proceed to single cell electroporation.
680	**CRITICAL STEP:** To avoid any contamination place forceps into the hot bead sterilizer for ~ 10 sec
681	before any handling of insert.
682	**CRITICAL STEP:** Work on an electrophysiology microscope setup in a laminar flow box (see
683	Equipment section) to prevent contamination.
684	51. Apply positive pressure to the pipette to approach a cell to electroporate. Monitor by audio
685	output of the Axoporator 800A amplifier the tip resistance of the electroporation pipette
686	throughout the entire procedure. The resistance should be between 10–15 MΩ.
687	**CRITICAL STEP:** Similarly to patch-clamp recording technique, positive pressure on the
688	electroporation pipette is maintained to keep the tip of the pipette clean while penetrating the
689	tissue.
690	**CRITICAL STEP:** For reproducible expression level of the plasmids between different
691	electroporation sessions, ensure that the pipette resistance is constant.
692	52. Move the tip of the electroporation electrode close to a cell of interest while reducing the
693	positive pressure.
694	53. Approach the cell without sealing the electrode with membranes from other cells in the tissue.
695	Touch the plasma membrane which causes a rise in tip resistance indicated by a rise in pitch.
696	Immediately release the pressure and wait for the resistance to increase to 25–40 MΩ. Do not
697	apply suction and avoid the formation of a GΩ seal.
698	54. Apply a pulse train (e.g., voltage: −12 V, frequency: 50 Hz, pulse width: 500 µs, train duration:
699	500 ms). The optimal settings may differ depending on the cell type to electroporate.
700	**CRITICAL STEP:** For more reproducible expression levels of the plasmids between different cells,
701	try to wait for the resistance to increase to a similar value before applying the pulse train.
702	55. Slowly retract the pipette and begin applying very light positive pressure once the pipette is
703	retracted 2–4 µm away from the soma. Increase the positive pressure at more considerable
704	distances from the electroporated cell in order to maintain the pipette tip clean. Using the same
705	electrode, repeat steps 51-55 for each cell to be electroporated.
706	56. Cover the chamber with a 60-mm dish and transfer back to the tissue culture hood. Remove all
707	transfection medium and return the insert to the slice culture medium. Typically, 2-4 days are
708	needed for optimal expression levels of GEGIs in hippocampal organotypic slices. However, the
709	optimal time for a cell to express a given plasmid before starting the experiment has to be
710	determined empirically [37].

Stimulating transfected neurons Timing 30-90 min per recording depending on slice quality, the number of cells expressing the electroporated plasmids and the length of the recording

713	57. Start temperature-controlled perfusion system and place the organotypic culture in the
714	recording chamber. Weigh down membrane patch with c-shaped gold wire.
715	**? TROUBLESHOOTING**
716	58. Tune the Ti:Sapph laser to 980 nm for simultaneous excitation of tdimer2 and GEGI.
717	**? TROUBLESHOOTING**

718   59. Approach a transfected CA3 neuron with the patch pipette, switching between red
719   epifluorescence and IR-Dodt contrast (CCD camera).
720   **? TROUBLESHOOTING**
721   60. Establish a GΩ-seal and break in to establish whole-cell configuration.
722   **CRITICAL STEP**: Stimulate an individual transfected cell to avoid stimulation of presynaptic
723   terminals close to the terminal under scrutiny. This will ensure that the GEGI transients originate
724   from the imaged terminal and are not a consequence of glutamate spillover.
725   61. Move the stage to center the objective on CA1. Search for red fluorescent axons using two-
726   photon excitation.
727   **? TROUBLESHOOTING**

728 **Imaging synaptic glutamate release**
729   62. Scan modality and signal analysis depend on the synaptic parameter under scrutiny. To localize
730   the fusion site, acquire fast frame scans followed by fitting with a Gaussian kernel (Option A). To
731   analyze the amplitude of glutamate transients, acquire spiral scans (Option B). To extract the
732   amplitude, define a region of interest in every trial and fit an exponential decay function to the
733   extracted time course.
734
735   (A) **Fusion site localization** Timing 1 hour per recording
736   i.   Inject current pulses (2-3 ms, 1.5-3.5 nA) into the soma and acquire rapid frame scans of a single
737   bouton (high zoom, 16 x 16 pixels, 1 ms/line).
738   ii.   Treat the raw images by a wavelet method to reduce photon shot noise [38] and improve SNR.
739   **? TROUBLESHOOTING**
740   iii.   Upsample the images to 128 x 128 pixels (Lanczos kernel).
741   iv.   Align the images using a Fast Fourier transform (FFT) performed on the red fluorescence signal
742   (tdimer2).
743   v.   Define a morphology mask to define a continuous area encompassing bouton and axon (pixel
744   intensity ≥ 10% to 30% maximal intensity).
745   vi.   Calculate the relative change in GEGI fluorescence ($\Delta F/F_0$) pixel by pixel using the mean of 5
746   baseline frames as F_0. Calculate the relative change and average the top 3% pixel values (of the
747   GEGI signal) within the bouton mask to obtain the peak amplitude.
748   vii.   Construct a template (2-D anisotropic Gaussian kernel) from the average of 5 trials classified as
749   success. A trial is classified as success when the peak amplitude is above 2σ of the baseline
750   frames.
751   viii.   Perform a first round of analysis where fitting the template to every single frame by adapting
752   only the amplitude and keeping the location and shape of the kernel fixed at the template values
753   to obtain a preliminary classification of 'successes' ($\Delta F/F_0 > 2\sigma$ of baseline noise) and 'failures'
754   ($\Delta F/F_0 < 2\sigma$ of baseline noise).
755   ix.   Repeat the fitting procedure on all trials classified as successes (step viii) allowing for variable
756   location in order to localize the fusion site
757   **? TROUBLESHOOTING**
758   x.   As a control, apply the same localization procedure to the failure trials and to the frame before
759   stimulation.

? TROUBLESHOOTING

761	(B) **Amplitude extraction and failure analysis** Timing 1 hour per recording

762	i.	Inject current pulses (2-3 ms, 1.5-3.5 nA) into soma and acquire rapid frame scans of a single
763		bouton (high zoom, 16 x 16 pixels, 1 ms/line).
764	ii.	If a bouton shows AP-induced fluorescence increase (green channel), switch to spiral scan mode.
765		**? TROUBLESHOOTING**
766	iii.	Acquire AP-induced GEGI transients at regular intervals (10 s), using 500 or 1000 Hz sampling.
767		Image only for the duration of the GEGI transients (~20 to 80 ms) to minimize laser exposition.
768	iv.	For amplitude extraction, linearize the spiral scans and display them as xt-plots (Fig. 5c).
769	v.	To distinguish successful glutamate release events from failures, perform a statistical comparison
770		of fluorescence fluctuations before stimulation (ΔF baseline, n = 64 columns/locations) and
771		response amplitude (ΔF response, n = 64 columns/locations). A significant difference suggests a
772		success, lack of significance a failure trial. This classification is preliminary; the final failure
773		analysis is performed after amplitude extraction (step xi).
774	vi.	As there may be lateral drift between individual trials, it is necessary to assign a new region of
775		interest (ROI) for each success trial. The spiral scan covering the entire bouton may hit the GEGI
776		transient once or several times per line. Sort the pixel columns (i.e., spatial positions) according
777		to the change in fluorescence (ΔF) in each column (Fig. 5d). In a given trial, only the columns
778		which display a clear change in fluorescence ($\Delta F > \frac{1}{2}$ max ΔF) are analyzed (ROI). The threshold is
779		once adjusted according to the noise of the imaging system but should be kept constant for
780		amplitude comparisons between different experiments.
781	vii.	In failure trials, evaluate identical columns/locations than in the last success trial.
782	viii.	If necessary, correct traces for GEGI bleaching (see Box 1).
783	ix.	For each bouton, extract the characteristic decay time constant (τ) by fitting a mono-exponential
784		function to the average GEGI fluorescence transient.
785	x.	Estimate the glutamate transient amplitude for every trial by fitting an exponential function to
786		the decay of the fluorescence transient (fixed τ, amplitude as the only free parameter).
787		**? TROUBLESHOOTING**
788	xi.	For each trial, determine the imaging noise (σ) from the baseline of the extracted fluorescence
789		time course. Classify as 'success' trials where average $\Delta F/F_0 > 2\sigma$ above baseline imaging noise,
790		otherwise classify as 'failure'.

Box 1: Bleaching of GEGI

792	During imaging, some GEGI molecules bleach, leading to a decrease in baseline fluorescence during each
793	trial (Supplementary Figure 1). This may cause problems when fitting an exponential function to the
794	decay of the glutamate response, since at least two time constants have to be taken into account. To
795	correct individual trials from one bouton for bleaching, fit an exponential decay function to the average
796	of several 'failure' trials. Subtract this function from each trial (failures and successes; step 63B viii).
797	Between trials, fluorescence partially recovers, indicating lateral diffusion of GEGI molecules in the
798	axonal membrane. Some loss of GEGI fluorescence (20-40%) during the course of the experiment can be

799 tolerated since it does not affect the glutamate-induced relative change in fluorescence ($\Delta F/F_0$,
800 Supplementary Figure 1). We found that manual refocusing between trials can lead to substantial
801 bleaching of the indicator. This can be minimized by automated refocusing between trials.

Troubleshooting

803 Step 57: Slices are contaminated. See [30] for proper slice culture handling.

804 Step 58: No cells express the construct. Ensure that the constructs are incorporated into the target cells
805 by adding a fluorescent dye such as Alexa Fluor 594 to the DNA mix (Step 47). After applying the pulse
806 train to the target neuron (Step 54), take a fluorescence image (e.g., Leica Z6 APO) to ensure that the
807 DNA solution and fluorescent dye were successfully electroporated. For more details for the
808 electroporation procedure refer to [37].

809 Step 59: Cells are dying after transfection with the constructs. Lower the expression of the GEGI, ensure
810 that the pipette resistance (Step 49) is not lower than 10-15 MΩ in the bath before electroporation,
811 and/or reduce expression time. A large pipette tip diameter (low resistance) can lead to overexpression
812 of the GEGI and cell toxicity. Cells should be imaged 2-4 days after electroporation, as longer expression
813 of GEGIs can affect cell health.

814 **CAUTION:** Very strong promoters (CMV) should not be used for physiological experiments in neurons.

815 Step 61: Slice is drifting, focus is not stable. Lower the perfusion rate. Check that the temperatures of the
816 perfusion solution and of the imaging chamber of the microscope are stable to avoid thermal expansion
817 during the experiment.

818 Step 62A (ii): The responses are very weak and barely above noise. Wait longer after electroporation for
819 a higher expression level. If the expression levels are too low, the GEGI signal from a single vesicle may
820 be below the detection limit. The detection limit is determined by the noise level of the optical recording
821 setup. Minimize background fluorescence, which can be caused by leaking room light, stray pump laser
822 photons (green), or excessive dark counts in aging PMTs. Condenser detection is sensitive to the
823 refractive index of the immersion oil and correct (Köhler) position.

824 Step 62A (ix): The localization seems inaccurate. Calibrate the optical and mechanical performance of
825 your system using fluorescent microbeads. Imaging of microbeads (0.17 µm diameter) positioned next to
826 a fluorescent presynaptic terminal allows quantifying the accuracy of the response localization
827 procedure.

828 Step 62A (x): In cases where the positions of apparent 'failures' clusters in a second area of the bouton,
829 exclude the bouton from further analysis as it might be a multi-synapse bouton.
830
831 Step 62B (ii): The success rate in finding a bouton releasing glutamate is very low. This can be due to low
832 release probability. Check [Ca^{2+}] of the ACSF.

833   Step 62B (x): In some trials, the baseline fluorescence may show large fluctuations caused by green
834   fluorescent vesicles passing through the axon. Remove these trials from further analysis.

835   **Timing**

836	Steps 1-4	Generation of GEGIs	7 days (5 h hands-on-time)
837	Steps 5-15	Expression and purification of new GEGIs	3 days (10 h hands-on-time)
838	Steps 16-20	Dynamic range determination	1 h
839	Steps 21-27	K_d determination	2h/ligand
840	Steps 28-32	Association kinetics	4 h/variant
841	Steps 33-37	Dissociation kinetics	1 h/variant
842	Steps 38-42	Determination of dynamic range and K_d in cells	2 days (5 h hands-on time)
843	Steps 43-44	Subcloning into neuronal expression vector	7 days (5 h hands-on time)
844	Step 45	Culture preparation	15 min/brain
845	Steps 46-47	Preparation of plasmids and DNA	10 min
846	Steps 48-56	Single-cell electroporation	10-20 min/slice
847	Steps 57-61	Stimulating transfected neurons	30-90 min/recording
848	Steps 62A (i-x)	Fusion site localization	1 h/recording
849	Steps 62B (i-xi)	Amplitude extraction and failure analysis	1h/recording

850   **Anticipated results**

851   **Assessing the properties of neighboring boutons**
852   Once a responding bouton is identified, several neighboring boutons along the same axon can be imaged
853   sequentially. Neighboring boutons frequently have similar release probabilities and response amplitudes
854   (Fig. 6a). In rare cases, however, we found dramatic differences in response amplitude between
855   neighboring boutons (Fig. 6b). To test whether boutons on the same axon are functionally similar, we
856   generated random pairs by drawing from our entire set of characterized boutons. The differences
857   between randomly selected boutons are normally distributed (black bars in Fig. 6d). The actual
858   difference between neighboring boutons (red line in Fig. 6d) is at the low end of the distribution,
859   indicating that neighboring boutons tended to have similar release probabilities. A similar result,
860   however non-significant, was found when response amplitudes were analyzed (Fig. 6e and f).

861   **Application of fast GEGIs**
862   While iGluSnFR has an excellent SNR, it is too slow to resolve vesicle fusion events during high-frequency
863   transmission [39]. Recently developed ultrafast GEGIs, iGlu$_u$ and iGlu$_f$ [13] resolve individual responses during
864   100 Hz trains, albeit with slightly lower SNR as shorter transients correspond to fewer photons collected
865   (Fig. 7a). For these experiments, scan speed was increased to 1 kHz, and a high Ca^{2+} solution was used to
866   increase release probability. Under these conditions, individual boutons typically had a release
867   probability of 1 on the first AP, which rapidly dropped to ~0.2 towards the end of the 100 Hz train. After
868   a brief recovery period (0.5 s), most boutons could restore their initial high release probability (Fig. 7b
869   and c). Interestingly, the depression also affected the amplitude of individual successes, suggesting a

870 switch from multivesicular release (MVR) to univesicular release during high-frequency activity [1,40].
871 Alternatively, a switch from full fusion to partial fusion of synaptic vesicles[41] could explain this
872 observation. Responses from an iGluSnFR-expressing bouton during high-frequency stimulation are
873 shown for comparison (blue traces, Fig. 7a). Summation of 100 Hz release events drives this slow GEGI
874 towards saturation, making it impossible to disentangle single-pulse responses by deconvolution. As
875 saline with high calcium concentration (4 mM) was used in these experiments, the prevalence of MVR
876 under more physiological conditions remains to be investigated. In this context, an important advantage
877 of GEGI measurements compared to GECIs[42] is their independence from extracellular $[Ca^{2+}]$, allowing to
878 investigate the impact of changes in $[Ca^{2+}]_e$ on presynaptic function[43]. In summary, ultrafast GEGIs allow
879 direct visualization of short-term plasticity at individual synapses and may help unraveling the underlying
880 biophysical mechanisms.

Data availability
882 The data that support the findings of this study are available from the corresponding author (Email:
883 thomas.oertner@zmnh.uni-hamburg.de) on request.

Author contributions
891 C.D.D., J.S.W, K.T., and T.G.O. designed the experiments and prepared the manuscript. C.D.D. performed
892 synaptic imaging experiments. N.H., S.K., C.C. and M.G. created and characterized novel iGluSnFR
893 variants, C.S. wrote software to acquire and analyze GEGI data.

Competing interest statement
895 The authors declare no competing interests.

References
897 1.　Pulido, C. & Marty, A. Quantal Fluctuations in Central Mammalian Synapses: Functional Role of
898 　Vesicular Docking Sites. *Physiol. Rev.* **97,** 1403–1430 (2017).

899 2.　Choquet, D. & Triller, A. The Dynamic Synapse. *Neuron* **80,** 691–703 (2013).

900 3.　Namiki, S., Sakamoto, H., Iinuma, S., Iino, M. & Hirose, K. Optical glutamate sensor for
901 　spatiotemporal analysis of synaptic transmission. *Eur. J. Neurosci.* **25,** 2249–59 (2007).

902 4.　Okubo, Y. *et al.* Imaging extrasynaptic glutamate dynamics in the brain. *Proc. Natl. Acad. Sci. U. S.*

903   *A.* **107,** 6526–31 (2010).

904   5.   Brun, M. A. *et al.* A semisynthetic fluorescent sensor protein for glutamate. *J. Am. Chem. Soc.* **134,**
905   7676–7678 (2012).

906   6.   Okumoto, S. *et al.* Detection of glutamate release from neurons by genetically encoded surface-
907   displayed FRET nanosensors. *Proc. Natl. Acad. Sci. U. S. A.* **102,** 8740–5 (2005).

908   7.   Tsien, R. Y. Building and breeding molecules to spy on cells and tumors. in *FEBS Letters* **579,** 927–
909   932 (2005).

910   8.   Hires, S. A., Zhu, Y. & Tsien, R. Y. Optical measurement of synaptic glutamate spillover and
911   reuptake by linker optimized glutamate-sensitive fluorescent reporters. *Proc. Natl. Acad. Sci. U. S.*
912   *A.* **105,** 4411–4416 (2008).

913   9.   Marvin, J. S. *et al.* An optimized fluorescent probe for visualizing glutamate neurotransmission.
914   *Nat. Methods* **10,** 162–170 (2013).

915   10.   Borghuis, B. G., Looger, L. L., Tomita, S. & Demb, J. B. Kainate Receptors Mediate Signaling in Both
916   Transient and Sustained OFF Bipolar Cell Pathways in Mouse Retina. *J. Neurosci.* **34,** 6128–6139
917   (2014).

918   11.   O'Herron, P. *et al.* Neural correlates of single-vessel haemodynamic responses in vivo. *Nature*
919   **534,** 378–382 (2016).

920   12.   Brunert, D., Tsuno, Y., Rothermel, M., Shipley, M. T. & Wachowiak, M. Cell-Type-Specific
921   Modulation of Sensory Responses in Olfactory Bulb Circuits by Serotonergic Projections from the
922   Raphe Nuclei. *J. Neurosci.* **36,** 6820–6835 (2016).

923   13.   Helassa, N. *et al.* Ultrafast glutamate sensors resolve high-frequency release at Schaffer collateral
924   synapses. *Proc. Natl. Acad. Sci. U. S. A.* **115,** 5594–5599 (2018).

925   14.   Wu, J. *et al.* Genetically Encoded Glutamate Indicators with Altered Color and Topology. *ACS*
926   *Chem Biol.* **13,** 1832–1837 (2018).

927   15.   Marvin, J. S. *et al.* Stability, affinity, and chromatic variants of the glutamate sensor iGluSnFR. *Nat.*
928   *Methods* **15,** 936–939 (2018).

929   16.   Miesenbock, G., De Angelis, D. A. & Rothman, J. E. Visualizing secretion and synaptic transmission
930   with pH-sensitive green fluorescent proteins. *Nature* **394,** 192–195 (1998).

931   17.   Granseth, B., Odermatt, B., Royle, S. J. & Lagnado, L. Clathrin-mediated endocytosis is the
932   dominant mechanism of vesicle retrieval at hippocampal synapses. *Neuron* **51,** 773–786 (2006).

933   18.   Fernández-Alfonso, T., Kwan, R. & Ryan, T. A. Synaptic Vesicles Interchange Their Membrane
934   Proteins with a Large Surface Reservoir during Recycling. *Neuron* **51,** 179–186 (2006).

935   19.   Voglmaier, S. M. *et al.* Distinct Endocytic Pathways Control the Rate and Extent of Synaptic Vesicle
936   Protein Recycling. *Neuron* **51,** 71–84 (2006).

937   20.   Li, H. Concurrent imaging of synaptic vesicle recycling and calcium dynamics. *Front. Mol. Neurosci.*
938   **4,** 1–10 (2011).

939 21. Li, Y. & Tsien, R. W. pHTomato, a red, genetically encoded indicator that enables multiplex
940   interrogation of synaptic activity. *Nat. Neurosci.* **15,** 1047–53 (2012).

941 22. Rose, T., Schoenenberger, P., Jezek, K. & Oertner, T. G. Developmental refinement of vesicle
942   cycling at Schaffer collateral synapses. *Neuron* **77,** 1109–21 (2013).

943 23. Balaji, J. & Ryan, T. A. Single-vesicle imaging reveals that synaptic vesicle exocytosis and
944   endocytosis are coupled by a single stochastic mode. *Proc. Natl. Acad. Sci.* **104,** 20576–20581
945   (2007).

946 24. Gandhi, S. P. & Stevens, C. F. Three modes of synaptic vesicular recycling revealed by single-
947   vesicle imaging. *Nature* **423,** 607–13 (2003).

948 25. Zhu, Y., Xu, J. & Heinemann, S. F. Synaptic vesicle exocytosis-endocytosis at central synapses.
949   *Commun. Integr. Biol.* **2,** 418–419 (2009).

950 26. Maschi, D. & Klyachko, V. A. Spatiotemporal Regulation of Synaptic Vesicle Fusion Sites in Central
951   Synapses. *Neuron* **94,** 65–73.e3 (2017).

952 27. Betz, W. J. & Bewick, G. S. Optical analysis of synaptic vesicle recycling at the frog neuromuscular
953   junction. *Science* **255,** 200–3 (1992).

954 28. Laviv, T. *et al.* Simultaneous dual-color fluorescence lifetime imaging with novel red-shifted
955   fluorescent proteins. *Nat. Methods* **13,** 989–992 (2016).

956 29. Campbell, R. E. *et al.* A monomeric red fluorescent protein. *Proc Natl Acad Sci U S A* **99,** 7877–
957   7882 (2002).

958 30. Gee, C. E., Ohmert, I., Wiegert, J. S. & Oertner, T. G. Preparation of Slice Cultures from Rodent
959   Hippocampus. *Cold Spring Harb. Protoc.* **2017,** pdb.prot094888 (2017).

960 31. Pologruto, T. A., Sabatini, B. L. & Svoboda, K. ScanImage: Flexible software for operating laser
961   scanning microscopes. *Biomed Eng Online* **2,** 13 (2003).

962 32. Suter, B. A. *et al.* Ephus: multipurpose data acquisition software for neuroscience experiments.
963   *Front. Neural Circuits* **4,** 1–12 (2010).

964 33. Negrean, A. & Mansvelder, H. D. Optimal lens design and use in laser-scanning microscopy.
965   *Biomed. Opt. Express* **5,** 1588–609 (2014).

966 34. Jensen, T. P., Zheng, K., Tyurikova, O., Reynolds, J. P. & Rusakov, D. A. Monitoring single-synapse
967   glutamate release and presynaptic calcium concentration in organised brain tissue. *Cell Calcium*
968   **64,** 102–108 (2017).

969 35. Hires, S. A., Zhu, Y. & Tsien, R. Y. Optical measurement of synaptic glutamate spillover and
970   reuptake by linker optimized glutamate-sensitive fluorescent reporters. *Proc Natl Acad Sci U S A*
971   **105,** 4411–4416 (2008).

972 36. de Lorimier, R. M. *et al.* Construction of a fluorescent biosensor family. *Protein Sci.* **11,** 2655–75
973   (2002).

974 37. Wiegert, J. S., Gee, C. E. & Oertner, T. G. Single-cell electroporation of neurons. *Cold Spring Harb.*
975   *Protoc.* **2017,** 135–138 (2017).

976 38. Luisier, F., Vonesch, C., Blu, T. & Unser, M. Fast interscale wavelet denoising of Poisson-corrupted
977   images. *Signal Processing* **90,** 415–427 (2010).

978 39. Taschenberger, H., Woehler, A. & Neher, E. Superpriming of synaptic vesicles as a common basis
979   for intersynapse variability and modulation of synaptic strength. *Proc. Natl. Acad. Sci.* **113,**
980   E4548–E4557 (2016).

981 40. Oertner, T. G., Sabatini, B. L., Nimchinsky, E. A. & Svoboda, K. Facilitation at single synapses
982   probed with optical quantal analysis. *Nat. Neurosci.* **5,** 657–64 (2002).

983 41. Grabner, C. P. & Moser, T. Individual synaptic vesicles mediate stimulated exocytosis from
984   cochlear inner hair cells. *Proc. Natl. Acad. Sci.* **115,** 12811–12816 (2018).

985 42. Helassa, N., Podor, B., Fine, A. & Török, K. Design and mechanistic insight into ultrafast calcium
986   indicators for monitoring intracellular calcium dynamics. *Sci. Rep.* **6,** 38276 (2016).

987 43. Zucker, R. S. & Regehr, W. G. Short-Term Synaptic Plasticity. *Annu. Rev. Physiol.* **64,** 355–405
988   (2002).

989 ## Figure legends

990 **Fig 1: Overview of the protocol workflow for the development of glutamate sensors and 2-**
991 **photon imaging of glutamate transients in individual synapses.**

992 **Fig 2: Characterization of GEGIs.**
993 (**a**) Left: Setup for affinity and selectivity determination. GEGI in assay buffer is placed into a fluorescence
994 cuvette with a magnetic stirrer and placed inside the sample chamber of the fluorescence spectrometer
995 (Fluorolog3, Horiba Scientific). With an Aladdin pump, the ligand (Glu, Asp, Ser) is continuously added to
996 the cuvette while the fluorescence is recorded (λ_{ex} = 492 nm, λ_{ex} = 514 nm). Right: Examples of affinity
997 curves of a GEGI for glutamate (black squares) and aspartate (black circles). The fluorescence emission is
998 corrected for dilution and bleaching and plotted against the glutamate concentration in the chamber.
999 The data is then fitted with a Hill equation (green and orange traces for glutamate and aspartate,
1000 respectively). (**b**) Left: Setup for stopped-flow kinetic measurement. The solutions are rapidly mixed in
1001 the mixing chamber and then pushed into the optical cell where the fluorescence is excited at 492 nm
1002 and emission is detected by a PMT with a cut-off filter (>530 nm). For association the GEGI in assay
1003 buffer without glutamate is loaded into the drive syringe B and mixed with assay buffer containing
1004 increasing concentrations of glutamate filled in drive syringe A. For dissociation the GEGI in assay buffer
1005 with saturating glutamate concentration is loaded into the drive syringe B and mixed with GluBP 600n in
1006 assay buffer filled into drive syringe A. For both measurements the PMT zero level is determined by
1007 mixing assay buffer with assay buffer and the intrinsic fluorescence of the GEGI is recorded by mixing the
1008 GEGI in assay buffer with assay buffer (both without Glu). Right: Examples for recorded time traces. Top:
1009 Fluorescence increase observed when GEGIs are mixed with increasing glutamate concentration.
1010 Bottom: Decrease in fluorescence when glutamate is retained from GEGI by GluBP 600n. The raw data
1011 are fitted with monoexponential decays (dark green line).

Fig 3: iGluSnFR expression in CA3 pyramidal cells in organotypic slice culture of rat hippocampus.

(**a**) Co-expression of two plasmids in individual CA3 pyramidal cells in organotypic slice culture. The red fluorescent protein tdimer2 labels the axoplasm while the membrane-anchored iGluSnFR is exposed to the extracellular space. (**b**) Transmitted light image (dark field) of a transfected organotypic culture merged with a wide-field fluorescence image showing three transfected CA3 neurons. The area for synaptic imaging is indicated (red dotted box). Scale bar represents 500 µm. (**c**) Two-photon image stack (maximum intensity projection) of CA3 axons in CA1 *stratum radiatum* (cells not identical to panel b). Scale bar represents 10 µm. Image from [13]. (**d**) Maximum intensity projection of two-photon images of CA3 pyramidal neuron expressing $iGlu_u$ 4 days after electroporation (fluorescence intensity is shown as inverted gray values). $iGlu_u$ shown here and other GEGIs had their fluorescence mainly localized to the plasma membrane over the entire cell. The scale bar represents 50 µm (left image) and 5 µm (right image). (**e**) Action potentials are elicited in a transfected neuron by somatic current injections and glutamate release is simultaneously optically recorded (GEGI fluorescence) from a single Schaffer collateral bouton in CA1, showing a broad distribution of amplitudes and occasional failures. Images were acquired at 500 Hz at 34°C. Individual trials are classified as successes if the peak amplitude of the GEGI transient is >2σ (green traces) and as failures when the peak amplitude is <2σ (gray traces). Note propagation delay between presynaptic APs and glutamate release events at distal bouton.

Fig 4: Localization of fluorescence transients in low and high $[Ca^{2+}]_o$.

(**a**) Morphology of individual boutons. Red fluorescence was upsampled (16 x 16 pixels to 128 x 128 pixels)**,** aligned and averaged over all trials. Scale bars represent 0.5 µm. (**b**) Average response of iGluSnFR superimposed with bouton outline (black line) from red channel (morphology). The bouton outline was generated by thresholding the red channel followed by smoothing. (**c**) Two-dimensional Gaussian fit to average response. On average, the full width at half maximum (FWHM) was 763 ± 29 nm (n = 12; 5 boutons shown here) (**d**) Plotting the center position of 2D Gaussian fits to individual trials. Fusion appears to be localized to a small region on the bouton (active zone). Amplitude ($\Delta F/F_0$) of individual trials is color-coded. Scale bars represent 0.5 µm. (**e**) Increasing the extracellular Ca^{2+} concentration increased the amplitude of individual responses, but did not lead to release events outside the active zone. (**f**) Fitting responses classified as failures (< 2σ of baseline noise) did not reveal any clustering, indicating that there was indeed no localized signal in these trials (true negatives). (**g**) Fitting frames before stimulation (green baseline fluorescence) did also not result in clustering.

Fig. 5: Signal extraction of GEGI transients from a single Schaffer collateral bouton in CA1.

(**a**) The spatial extent of iGluSnFR fluorescence transients was 760 nm, on average (FWHM, short axis of Gaussian fits). No deconvolution was applied. (**b**) Sampling the surface of the bouton by traditional raster scanning requires extreme acceleration of the scan mirrors at the turning points, leading to large positional errors. Spiral scans avoid sharp direction changes (no flyback) and can, therefore, sample the entire bouton surface in 1 or 2 ms. Due to the elongated PSF (1.8 µm in the axial direction), upper and lower surface of a bouton are sampled simultaneously. (**c**) Plotting the unfolded spiral scan lines vs. time (single trial). Raw fluorescence intensity is coded in pseudocolors. At t = 58 ms, a glutamate release event from an individual presynaptic terminal occurred and was sampled twice during every spiral scan. (**d**) Only columns with ΔF > ½ max (ΔF) were analyzed (ROI, region of interest). Green trace: Extracted

1053   fluorescence transient (before bleach correction). (**e**) *Upper panel:* Average of 10 trials (single APs) to
1054   analyze lateral spread of signal from t=0 to t=18 ms. *Lower panel:* Decay of fluorescence transient (5 scan
1055   lines plotted = 18 ms). Note the lack of lateral spread of the signal due to slow diffusion of membrane-
1056   anchored GEGI. (**f**) iGluSnFR response amplitude (green markers) of a single bouton stimulated with
1057   single APs every 10 s. Note that response amplitudes were constant over time. A time window before
1058   stimulation was analyzed to estimate imaging noise (gray markers). The histogram of response
1059   amplitudes shows separation between failures of glutamate release (overlap with the baseline
1060   histogram) and successes.

1061   **Fig. 6: Release statistics of neighboring boutons on the same axon.**
1062   (**a**) Glutamate transients (green dots) and baseline fluorescence (grey dots) of two neighboring boutons
1063   measured in ACSF containing 2 mM Ca^{2+} and 1 mM Mg^{2+} located on the same axon (left panels) and their
1064   corresponding histogram counts (right panels). (**b**) Glutamate transients (blue dots) and baseline
1065   fluorescence (grey dots) of two neighboring boutons located on the same axon (left panels) and their
1066   corresponding histograms (right panels) measured in ACSF containing 2 mM Ca^{2+} and 1 mM Mg^{2+} and
1067   their corresponding histogram counts (right panels). (**c**) Synaptic release probability (p_r) (calculated out
1068   of ~ 100 trials) of individual boutons (B1) and their neighboring bouton on the same axon (B2); n=10. The
1069   pair of neighboring boutons from (a) and (b) are shown in green and blue, respectively. (**d**) Histogram of
1070 $\Delta\,p_r = |p_r BX - p_r BY|$. BX and BY are randomly paired from the dataset in (c). $|\Delta p_r B2 - \Delta p_r B1|$ (red vertical
1071   line) is significantly more similar than mean $\Delta\,p_r$ of two boutons paired randomly from the same dataset;
1072   (p-value: 0.0148). (**e**) Amplitude of the iGluSnFR signal given a success of a bouton B1 and its neighbor on
1073   the same axon (B2); n=10. The pair of neighboring boutons from (a) and (b) are shown in green and blue,
1074   respectively. (**f**) Histogram count of the difference between the average $\Delta F/F_0$ of successes only of two
1075   random neighboring boutons. The difference of the average $\Delta F/F_0$ of successes from two neighboring
1076   boutons (red vertical line) is not significantly more similar than the randomly connected pairs of boutons.
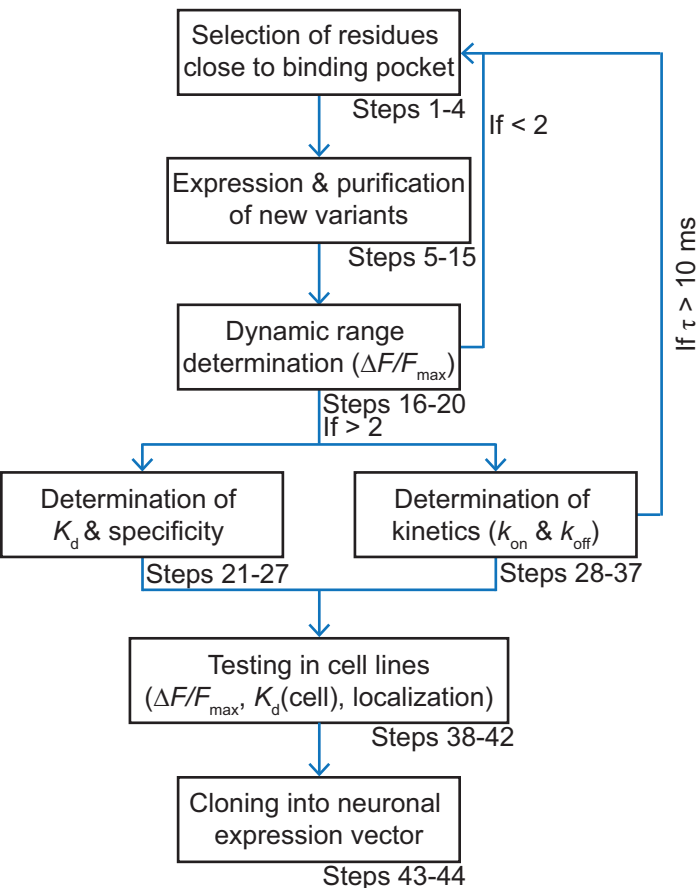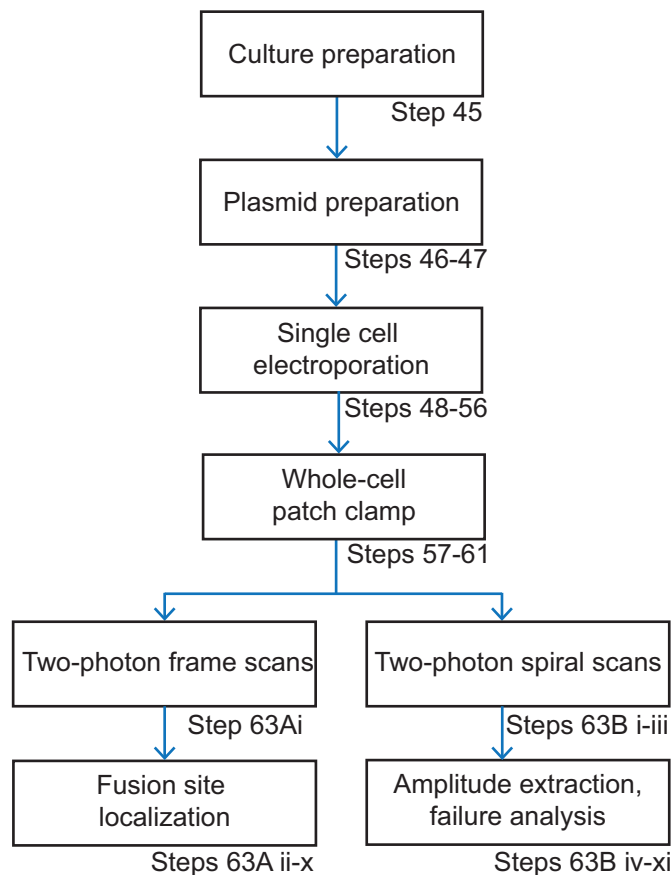
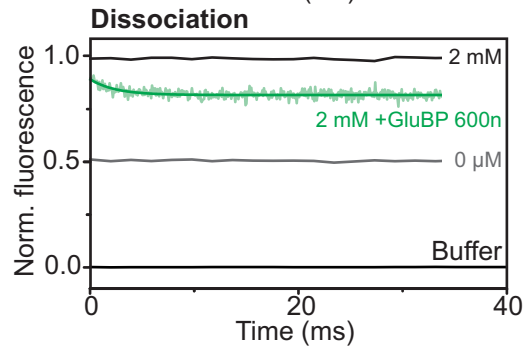1077   **Fig. 7: Resolving high-frequency transmission with ultrafast GEGI, iGlu$_u$.**
1078   (**a**) The presynaptic neuron was driven to spike at 100 Hz (10 APs). After a pause of 0.5 s, one more AP
1079   was triggered to quantify recovery from depression. iGluSnFR signals (blue) or iGlu$_u$ signals (green) were
1080   recorded at single Schaffer collateral boutons (only during the 100 Hz train) in *stratum radiatum*.
1081   Recordings were performed in 4 mM Ca^{2+} and 1 mM Mg^{2+} to ensure very high release probability. Note
1082   summation and saturation of iGluSnFR (but not iGlu$_u$) during the high-frequency train. (**b**) iGlu$_u$ responses
1083   to the 1st AP of the 100 Hz train, to the 9th AP of the train, and to the recovery pulse. To minimize
1084   bleaching, the bouton was only imaged (spiral scans) during pulses 1, 9 and 11. Note frequent failures in
1085   response to pulse 9. (**c**) Extracted single-trial amplitudes reveal strong depression and full recovery of
1086   this bouton. Failures of glutamate release can be seen in response to pulse 9. Note the large amplitude
1087   of initial responses compared to depressed responses. Plots were generated with violinplot.m (GitHub,
1088   ©Bastian Bechtold).

1089

1090   **SUPPLEMENTARY MATERIAL**

1091   -   **Supplementary Figure 1**

a **Flowchart of sensor development**

b **Flowchart of fast imaging in hippocampal slices**

Selection of residues close to binding pocket
Steps 1-4

If < 2

If τ > 10 ms

Expression & purification of new variants
Steps 5-15

Dynamic range determination ($\Delta F/F_{max}$)
Steps 16-20
If > 2

Determination of K_d & specificity
Steps 21-27

Determination of kinetics (k_{on} & k_{off})
Steps 28-37

Testing in cell lines ($\Delta F/F_{max}$, K_d(cell), localization)
Steps 38-42

Cloning into neuronal expression vector
Steps 43-44

Culture preparation
Step 45

Plasmid preparation
Steps 46-47

Single cell electroporation
Steps 48-56

Whole-cell patch clamp
Steps 57-61

Two-photon frame scans
Step 63Ai

Two-photon spiral scans
Steps 63B i-iii

Fusion site localization
Steps 63A ii-x

Amplitude extraction, failure analysis
Steps 63B iv-xi

a

Syringe pump

Ligand solution in basic buffer

Xe lamp

Excitation monochromator

492 nm

514 nm
Emission monochromator

PMT

Sample chamber with cuvette and magnetic stirrer

— Aspartate
— Glutamate

Bound fraction

[Ligand] (mM)

b

$\lambda_{em} > 530$ nm

$\lambda_{ex} = 492$ nm

Optical cell

Mixer

Drive syringe A

Drive syringe B

Stop syringe

Drive

Association

Norm. fluorescence

17.5 mM
3.13 mM
1.5 mM
750 µM
375 µM
0 µM

Buffer

Time (ms)

Dissociation

Norm. fluorescence

2 mM

2 mM +GluBP 600n

0 µM

Buffer

Time (ms)

a N—syn1—[iGluSnFR]—C 67%
N—syn1—[tdimer 2]—C 33%

b CA1
CA3   DG

c

e whole cell patch clamp   60x 1.0 NA

d

soma   50 mV
        5 ms

bouton   50% ΔF/F₀
          5 ms

	a	**b** Mean successes	**c** Gaussian fit	**d** Successes 1 mM Ca^{2+}	**e** Successes 4 mM Ca^{2+}	**f** Failures	**g** Baseline noise

Bouton 1 — av. $\Delta F/F_0$: 0.46 — av. $\Delta F/F_0$: 0.91

Bouton 2 — av. $\Delta F/F_0$: 0.42 — av. $\Delta F/F_0$: 0.81

Bouton 3 — av. $\Delta F/F_0$: 0.47 — av. $\Delta F/F_0$: 1.88

Bouton 4 — av. $\Delta F/F_0$: 0.49 — av. $\Delta F/F_0$: 0.91

Bouton 5 — av. $\Delta F/F_0$: 0.27 — av. $\Delta F/F_0$: 0.35

a iGluSnFR signal

760 nm FWHM

b Frame scan   Spiral scan

1 µm

1.7 µm

c Position along scan path

Spiral scan path

Release of glutamate

20 ms

Intensity (a.u.)

d Sorted columns

20 ms

20 ms

50 % ΔF/F₀

ROI

e

t=0

t=18 (ms)

Intensity (a.u.)

Position along scan path (pixels)

t=0 ms
t=6 ms
t=12 ms
t=14 ms
t=18 ms

f

ΔF/F₀ [%]

stimulation number

Counts

Response
Baseline

ΔF/F₀ [%]

a Axon 1

Bouton 1 | Bouton 2

b Axon 2

Bouton 1 | Bouton 2

a

1 2 3 4 5 6 7 8 9 10   500 ms   11

40 mV
10 ms

100%
$\Delta F/F_0$
10 ms

iGluSnFR

50 %
$\Delta F/F_0$
10 ms

iGlu$_u$

b

2 ms

50 %
$\Delta F/F_0$

Pulse 1   Pulse 9   Pulse 11

c

$\Delta F/F_0$ [%]

Pulse 1   Pulse 9   Pulse 11